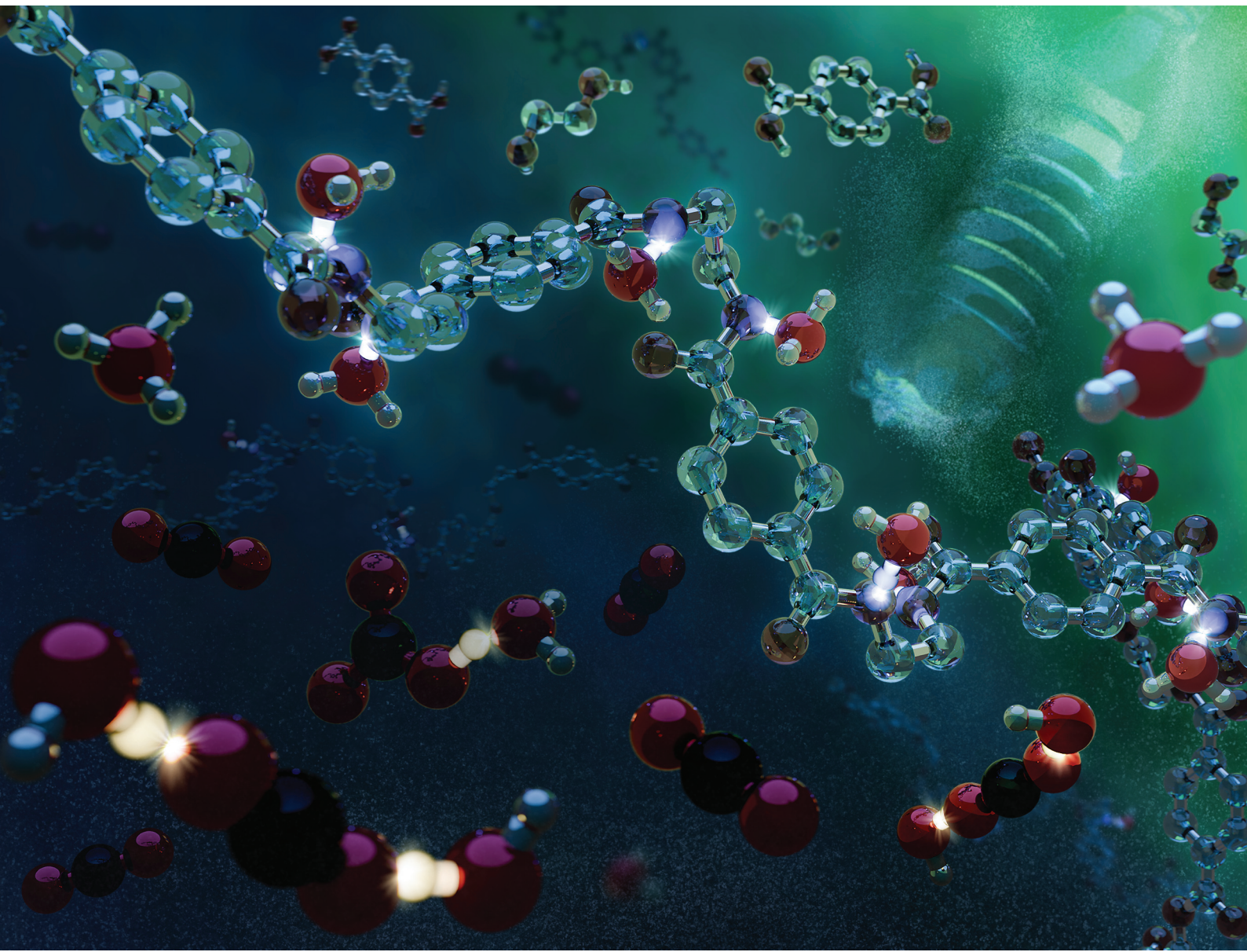


Green Chemistry

Cutting-edge research for a greener sustainable future

rsc.li/greenchem



ISSN 1463-9262



Cite this: *Green Chem.*, 2024, **26**, 6436

Subcritical CO_2 – H_2O hydrolysis of polyethylene terephthalate as a sustainable chemical recycling platform†

Dacosta Osei,^{a,b,c} Lakshmiprasad Gurrala,^{id a,b} Aria Sheldon,^{a,b} Jackson Mayuga,^{a,b} Clarissa Lincoln,^{d,e} Nicholas A. Rorrer^{id d,e} and Ana Rita C. Morais^{id *a,b}

The development of an efficient and environmentally sustainable chemical hydrolysis process for recycling waste plastics, based on green chemistry principles, is a key challenge. In this work, we investigated the role of subcritical CO_2 on the hydrolysis of polyethylene terephthalate (PET) into terephthalic acid (TPA) at 180–200 °C for 10–100 min. The addition of CO_2 into the reaction mixture led to the *in situ* formation of carbonic acid that helps to catalyze PET hydrolysis relative to hot compressed H_2O (i.e. N_2 – H_2O). The highest TPA yield of $85.0 \pm 1.3\%$ was obtained at 200 °C, PET loading of 2.5 g PET in 20 mL H_2O for 100 min, and 208 psi of initial CO_2 pressure. In addition, the subcritical CO_2 – H_2O system demonstrated high selectivity toward hydrolyzing PET in a mixture with polyethylene (PE) at 200 °C for 100 min, thus providing “molecular sorting” capabilities to the recycling process. The robustness of the process was also demonstrated by the ability to hydrolyze both colored Canada Dry and transparent Pure Life® waste PET bottles into high yields of TPA (>86%) at 200 °C. In addition, subcritical CO_2 – H_2O hydrolysis of colored PET bottles resulted in a white TPA product similar to that generated from transparent PET bottles. Overall, this work shows that, under optimized reaction conditions, subcritical CO_2 can provide acid tunability to the reaction medium to favor waste PET hydrolysis for subsequent recycling.

Received 23rd November 2023,
Accepted 6th February 2024

DOI: 10.1039/d3gc04576e
rsc.li/greenchem

1. Introduction

Plastics have become a common commodity in the global market and are indispensable to our society. The current worldwide production of polyethylene terephthalate (PET) is exceeding 82 million metric tons per year.¹ Despite their widespread use, PET mechanical recycling rates in the US are <19% and about 80% of waste PET is landfilled.² To address this issue, various chemical recycling processes (including solvolysis and thermal depolymerization approaches) have been actively developed over the past years to produce monomers from end-of-life PET.^{3–5} The produced and purified monomers can undergo repolymerization to produce recycled PET with virgin-like properties.⁴

Hydrolysis of PET into terephthalic acid (TPA) and ethylene glycol (EG) has received increasing attention because TPA is the major component in commercial production of PET.⁶ In the case of acid hydrolysis, mineral acids, such as concentrated H_2SO_4 and HNO_3 , are used.^{7–9} However, the major limitations associated with the mineral acid-catalyzed hydrolysis are severe corrosion issues, the need for highly polar solvents for TPA recrystallization, and generation of both inorganic salts and deleterious wastes.^{10,11} Another important limitation associated with H_2SO_4 -catalyzed hydrolysis is the carbonization of the products, notably EG, induced by the strong dehydrating effect of the acid, leading to lower reaction yields.¹¹

Neutral hydrolysis is an environmentally-friendly alternative to acid hydrolysis as it is performed using steam or water in the presence of water-soluble salts.^{5,12} Pereira *et al.* studied the performance of H_2O at varying temperatures (190–400 °C) and pressures (1–35 MPa) on the hydrolysis of both solid and molten PET.¹³ A high TPA yield (>85%) was observed when molten PET was hydrolyzed in saturated liquid H_2O (311 °C, 10 MPa and 30 min of reaction time). The cleavage of ester bonds by H_2O is promoted by the development of acidity at high temperatures.¹⁴ Marshal and Frank reported that the ion product (K_w) of H_2O increases with temperature and reaches a maximum of 6.34×10^{-12} , which results in a pH of 5.5 at 220 °C.¹⁵ Significantly faster hydrolysis rates have been

^aDepartment of Chemical and Petroleum Engineering, University of Kansas, Lawrence, Kansas 66045, USA. E-mail: ana.morais@ku.edu

^bWonderful Institute for Sustainable Engineering, University of Kansas, Lawrence, Kansas, 66045, USA

^cCenter for Environmentally Beneficial Catalysis, University of Kansas, Lawrence, Kansas 66047, USA

^dRenewable Resources and Enabling Sciences Center, National Renewable Energy Laboratory, Golden, CO, 80401, USA

^eBOTTLE Consortium, Golden, CO 80401, USA

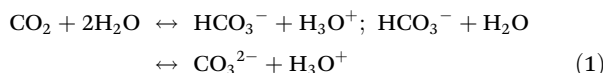
† Electronic supplementary information (ESI) available. See DOI: <https://doi.org/10.1039/d3gc04576e>



reported for molten PET than PET in the solid state; thus, reactions performed at temperatures greater than the melting temperature (T_m) of the substrate are highly recommended.^{5,16} Campanelli *et al.* reported that complete hydrolytic depolymerization of PET into monomer was achieved at 265 °C and with a H₂O:PET ratio >5:1 w/w. However, lower H₂O loadings (H₂O:PET ratio of 2:1 w/w) resulted in incomplete depolymerization due to the establishment of equilibrium conditions.¹⁷ It is worth mentioning that neutral hydrolysis requires high temperatures (>250 °C) and pressures (1–45 MPa),¹⁸ and long reaction times.^{13,16,19} In addition, the TPA produced through neutral hydrolysis has a considerably lower purity than that produced by acid hydrolysis. This is because impurities present in the waste PET, including dyes, pigments, metal catalysts, dicarboxylic acids, *etc.*, are not easily separated from the TPA during reaction, and additional purification steps are required.^{5,11}

The aforementioned shortcomings associated with both acid and neutral hydrolysis can be alleviated by the use of CO₂. CO₂ is known as a green chemical because it is nonflammable, nontoxic and readily available, and it is applied in diverse applications.^{5,20,21} One of them is its use in polymer modification.^{22–24} Due to its plasticization effect, the dissolution of CO₂ in polymers alters their properties at both the glassy and rubbery states, promotes swelling,^{25–27} and depresses both glass transition and crystallization temperature,^{28–30} which can lead to crystallization of amorphous regions within the polymer.³¹ Another application is the use of CO₂ for chemical deconstruction of plastics.^{32–36} For instance, Liu and Yin reported that the addition of CO₂ to the supercritical methanolysis of PET resulted in superior dimethyl terephthalate (DMT) yields (up to 95%) relative to the process without CO₂.³² Recently, Yu *et al.* reported that the addition of 2 MPa of CO₂ to the ethanolysis of PET resulted in 37% higher product yield in comparison with CO₂-free ethanolysis.³⁴ Li *et al.* investigated the mechanism of hydrolysis of waste PET bottles in the presence of a solid super-acid catalyst (SO₄²⁻/TiO₂) and supercritical CO₂ (scCO₂) and reported that scCO₂ improve the efficiency of the process due to its ability to carry more H₂O and H₃O⁺ inside the substrate.³⁷ Also, the hydrolysis of waste bottle PET in WO_x/TiO₂ solid acid catalysts and scCO₂ was investigated by Guo *et al.*, who reported that scCO₂ promotes the swelling of the substrate and carries H₂O and hydronium ions into the amorphous region of PET matrix.³³

The dissolution of CO₂ in H₂O provides a tunable acidic medium through the generation of carbonic acid (H₂CO₃) *in situ*, which loses protons to form bicarbonate (HCO₃⁻) and later carbonate (CO₃²⁻) anions,³⁸ according to the following equations:



The acidity of the subcritical CO₂-H₂O system is influenced by the solubility of CO₂ and dissociation of H₂CO₃ in H₂O.³⁸

Hunter and Savage reported that at temperatures >150 °C, the solubility of CO₂ (at given amount) in H₂O increases with increasing temperature, while the dissociation of H₂CO₃ in H₂O decreases with temperature.³⁸ Thus, overall temperature dependence of pH in the CO₂-H₂O system is much more influenced by the temperature dependence of first dissociation constant (K_a) than the temperature dependence of dissolution of CO₂ in H₂O. This indicates that the addition of CO₂ will be mostly effective in inducing acid-hydrolysis of PET at temperatures between 150 and 200 °C.³⁸ At constant temperature, the extent of CO₂ dissolution in H₂O increases with increasing pressure. Thus, through thermodynamic fine-control (*i.e.* temperature, pressure and composition), the CO₂-H₂O reaction mixture can reach pH values low enough to induce cleavage of acid-labile ester bonds and provide reaction rates that are greater than those that occur in hot compressed H₂O (no added CO₂) reactions. Unlike mineral acid-catalyzed hydrolysis, the acidity of the medium generated by the addition of CO₂ does not represent an issue, as the pH of the system increases when CO₂ is released.²⁰ In addition, no neutralization waste is produced as CO₂ can be easily recovered and reused, and equipment corrosion issues are reduced relative to mineral acids.²⁰

Although the use of subcritical CO₂-H₂O mixture for the processing of many different biomasses (*e.g.*, wheat straw, elephant grass) has been widely reported by our group^{20,39–43} and other authors,^{44–46} to the best of our knowledge, this technology has been scarcely applied to waste plastics, such as PET. In this work, the feasibility of subcritical CO₂-H₂O mixture to catalyze the hydrolysis of PET was investigated. The effect of key operational conditions, including CO₂ pressure, temperature and residence time on the hydrolysis performance was investigated to identify optimal conditions. Further, the potential of this process to selectively hydrolyze PET within a mixture with other plastics (such as PE), and its robustness to handle real waste PET substrates (colored and transparent waste PET bottles) was scrutinized.

2. Experimental section

2.1. Materials

Granular semicrystalline PET (3–5 mm, product code: ES30-GL-000115), powder semicrystalline PET (300 µm, product code: ES30-PD-000132), amorphous PET film (product code: ES30-FM-000145) and polyethylene (150 µm, product code: ET30-PD-000110) were procured from Goodfellow Corporation (Pittsburgh, PA, USA). Amorphous PET film was cut into squares of 1 × 1 cm dimensions before cryogrinding. Colored Canada Dry soda, Mountain Dew® and Twist Up and transparent Pure Life® PET bottles were used as examples of colored and transparent waste PET bottles, respectively. The bottles were thoroughly washed and dried before usage. Terephthalic acid (TPA, purity = 99%, #CAS 100-21-0) was obtained from ACROS Organics (ThermoFisher Scientific, Waltham, MA, USA). Mono (2-hydroxyethyl) terephthalate (MHET) (95%



purity, #CAS 1137-99-1) was purchased from AmBeed (Arlington Heights, IL, USA). Bis(2-hydroxyethyl) terephthalate (BHET) (#CAS 959-26-2), dimethyl sulfoxide (DMSO) (HPLC grade, #CAS 67-68-5), methanol (HPLC grade, #CAS 67-56-1), formic acid (FA) (99% purity, #CAS 64-18-6) sodium hydroxide (#CAS 1310-73-2), acetonitrile (CH_3CN) (HPLC grade, #CAS 75-05-8), and hydrochloric acid (#CAS 7647-01-0) were obtained from Sigma-Aldrich (St Louis, MO, USA). The carbon dioxide (CO_2) and nitrogen (N_2) of research purity was procured from Matheson (Irving, TX, USA). All the chemicals were used as-received.

2.2. PET feedstock preparation

Granular semicrystalline PET was used directly with no additional sample preparation. Amorphous PET, colored Canada Dry and transparent Pure Life® waste PET bottles, and colored waste PET Mountain Dew and Twist Up bottles were cryoground in a SPEX SamplePrep 6770 Freezer mill at conditions of 10 counts per second (CPS), 10 min precooling, 1 min run time and 1 min cooling. This procedure was performed until a particle size $<300\text{ }\mu\text{m}$ was achieved. Then, after cryogrinding, cryoground samples were sieved using a Retsch vibratory sieve shaker (AS 200) by combining two sieves (American Standard Test Sieve Series) of different sizes (*i.e.* 106 μm and 300 μm) to obtain a particle size between 106 and 300 μm . Similarly, the pristine powder PET was also sieved between 106 and 300 μm . The sieved samples were then stored in sealed glass bottles at room temperature.

2.3. Subcritical $\text{CO}_2\text{-H}_2\text{O}$ hydrolysis

Subcritical $\text{CO}_2\text{-H}_2\text{O}$ hydrolysis experiments were carried out using a 100 mL Series 4590 micro stirred reactor from Parr Instrument Company (Moline, IL, USA), equipped with a thermocouple, flour-blade turbine impeller, heating jacket, and pressure transducer. Temperature and pressure were controlled using a Parr PID controller (4848). The reactions were carried out at varying temperatures, notably 180, 190 and 200 $^{\circ}\text{C}$, initial CO_2 pressures ranging from 108 to 408 psi and up to 100 min of residence time. The PET-to- H_2O loading of 1 : 8 (w/w) and an agitation speed of 400 rpm were maintained constant in all experiments. Prior to the reaction, the autoclave was flushed 3 times with CO_2 or N_2 . Upon reaching set reaction times, the reactor was rapidly cooled down using a water bath to quench the reaction and CO_2 (or N_2) was released when the reactor reached room temperature. The reactor contents were filtered under vacuum (Millipore vacuum pump, model no. WP6111560), using a Whatman filter paper (47 mm diameter and 0.2 μm pore size), and the volume of the post-reaction liquid fraction was measured. 200 μl of the filtrate was diluted in 25 mL of DMSO and analyzed by High-Pressure Liquid Chromatography (HPLC). Because the TPA is insoluble in H_2O at room temperature, the solid fraction, which included leftover PET, TPA and other H_2O -insoluble products, was dried in a vacuum oven 40 $^{\circ}\text{C}$ for 48 h. The dried insoluble solids were further dissolved in DMSO, and filtered to separate the solid leftover PET from DMSO-soluble products (*e.g.* TPA,

MHET, BHET, among others). The DMSO-soluble products were analyzed by HPLC, while the DMSO-insoluble fraction was dried in a vacuum oven at 40 $^{\circ}\text{C}$ for 48 h. Both liquid and solid fractions were analyzed using the procedures presented below. To analyze the structure and purity of the TPA produced from waste colored PET bottle using subcritical $\text{CO}_2\text{-H}_2\text{O}$, TPA was firstly separated from other insoluble products. Initially, the post-reaction solid fraction was dried in a vacuum oven at 40 $^{\circ}\text{C}$ for 48 h. The dried solid fraction was dissolved in 1 M NaOH to form a solution of sodium terephthalate (NaTPA) and filtered. 1 M HCl was added to the filtrate to reprecipitate TPA. TPA was then thoroughly washed with distilled H_2O , and dried in a vacuum oven at 40 $^{\circ}\text{C}$ for 48 h.

2.4. Combined severity factor

Combined severity factor (CS_{pCO_2}) includes the effect of multiple $\text{CO}_2\text{-H}_2\text{O}$ parameters, including temperature, CO_2 pressure, and reaction time into a single equation.⁴⁷ It has been applied to optimize the impact of temperature, reaction time and pH on the reaction outcomes as follows:³⁹

$$\text{CS}_{p\text{CO}_2} = \log(R_0) - \text{pH} \quad (2)$$

Overend and Chornet developed a model where both temperature and residence time are combined into a single severity factor (R_0), equivalent to the logarithmic form of eqn (3):⁴⁸

$$R_0 = \int_0^t e^{\left(\frac{T-T_0}{14.75}\right)} dt \quad (3)$$

where R_0 is the reaction ordinate, T is temperature in $^{\circ}\text{C}$, 14.75 is the activation energy under the operational conditions where the reaction obeys Arrhenius law and follows kinetics of first order, T_0 is the reference temperature assigned as 100 $^{\circ}\text{C}$, and t is residence time in min.^{49,50} To account for the addition of CO_2 and its impact on the *in situ* pH, the pH was calculated according to the following expression developed by Walsum:⁴⁷

$$\text{pH} = 8.00 \times 10^{-6} \times T^2 + 0.00209 \times T - 0.216 \times \ln(p_{\text{CO}_2}) + 3.92 \quad (4)$$

where T is temperature ($^{\circ}\text{C}$) and p_{CO_2} is partial pressure of CO_2 (atm). To calculate the partial pressure of CO_2 , the Henry's constant for $\text{CO}_2\text{-H}_2\text{O}$ mixture was used.⁴⁷ The solubility of CO_2 in H_2O at varying temperatures and pressures was determined using ASPEN Plus. CS_{pCO_2} factor has been extensively applied in the field of biomass processing,^{39,40,47,51} and its applicability for CO_2 -catalyzed hydrolysis of PET will be for the first time evaluated in this work.

2.5. Characterization of the liquid fraction

The liquid fraction samples were analyzed using a HPLC equipped with an Phenomenex Luna® 5 μm C18 (100 \AA , 150 \times 4.6 mm column, Part #00F-4252-E0) at 40 $^{\circ}\text{C}$ and 0.6 mL min $^{-1}$ flow rate with UV detector at 240 nm.⁵² A gradient mobile phase (a combination of 1 wt% FA and CH_3CN) was used with 99% FA and 1% CH_3CN and finishing at 60% FA and 40 wt% CH_3CN in 40 min. The theoretical yield of TPA,

BHET and MHET was calculated using external calibration curves performed by measuring the response of the respective standard compound of known concentration. The theoretical yield of TPA in the loaded PET was calculated by considering the molecular weight fraction of TPA within the PET monomer unit ($C_{10}H_8O_4$), which has a molar mass of 192 g mol^{-1} . Similarly, for BHET and MHET, a 254.2 and 210.2 g mol^{-1} of molar mass was used, respectively. The formulas below were used to calculate the yield of each product:

$$\text{TPA yield} = \frac{\text{mass of TPA obtained}}{\text{theoretical mass yield of TPA from initial PET}} \times 100 \quad (5)$$

$$\text{BHET yield} = \frac{\text{mass of BHET obtained}}{\text{theoretical mass yield of BHET from initial PET}} \times 100 \quad (6)$$

$$\text{MHET yield} = \frac{\text{mass of MHET obtained}}{\text{theoretical mass yield of MHET from initial PET}} \times 100 \quad (7)$$

PET conversion was calculated as follows:

$$\text{PET conversion}(\%) = \frac{\text{mass of initial PET} - \text{mass of unreacted PET (DMSO-insoluble)}}{\text{mass of initial PET}} \times 100 \quad (8)$$

Unknown peaks found in HPLC chromatograms were identified through Liquid Chromatography-Mass Spectrometry (LC-MS). LC-MS spectra were acquired on a Waters Acuity UPLC HClass equipped with a Waters QDa Mass Detector using a XBridge Peptide BEH C18 XP Column (130 \AA , $2.5\text{ }\mu\text{m}$, $4.6\text{ mm} \times 150\text{ mm}$) using a linear gradient of $95:5\text{ H}_2\text{O/0.1\% FA:CH}_3\text{CN/0.1\% FA}$ to $5:95\text{ H}_2\text{O/0.1\% FA:CH}_3\text{CN/0.1\% FA}$. Mass spectra were acquired in ESI- and UV traces were recorded at 254 nm .

2.6. Characterization of solids before and after depolymerization

2.6.1. Size exclusion chromatography. Weight average molar mass (M_w) and number average molar mass (M_n) values of pristine granular semicrystalline PET ($M_w = 43.9\text{ kDa}$, $M_n = 32.1\text{ kDa}$), ground colored Canada Dry ($M_w = 48.6\text{ kDa}$, $M_n = 35.5\text{ kDa}$), Mountain Dew® ($M_w = 49.0\text{ kDa}$, $M_n = 33.8\text{ kDa}$) and Twist Up ($M_w = 50.4\text{ kDa}$, $M_n = 36.0\text{ kDa}$) and transparent Pure Life® waste ($M_w = 37.4\text{ kDa}$, $M_n = 27.6\text{ kDa}$) PET bottles were determined by Size Exclusion Chromatography with Multi-Angle Light Scattering (SEC-MALS). SEC-MALS analysis was performed using a 1260 Infinity II LC system (Agilent), three sequential PL HFIPgel $250 \times 4.6\text{ mm}$ columns (Agilent), and a matching guard column. $1,1,1,3,3,3$ -Hexafluoroisopropanol (HFIP, Chem-Impex) was filtered through a $0.1\text{ }\mu\text{m}$ polytetrafluoroethylene (PTFE) filter,

amended with 20 mM sodium trifluoroacetate (NaTFAc, Sigma Aldrich, 98% purity), and used as the mobile phase. Samples were dissolved in this same solvent at a concentration of approximately 5 mg mL^{-1} , then pushed through $0.2\text{ }\mu\text{m}$ PTFE syringe filters. The HPLC operating conditions included a flow rate of 0.35 mL min^{-1} , a sample injection volume of $100\text{ }\mu\text{L}$, and the Multicolumn Thermostat (MCT) held at $40\text{ }^\circ\text{C}$. Detectors consisted of a miniDAWN TREOS Multi-Angle Light Scattering (MALS) detector (Wyatt Technology) used in combination with a Optilab T-rEX Differential Refractive Index detector (Wyatt Technology). All calculations were performed using a differential refractive index (dn/dc) value of 0.257 for PET in HFIP,⁵³ and Astra software (Wyatt Technology) was used for all data analysis.

2.6.2. Thermogravimetric analysis (TGA) and differential scanning calorimetry (DSC). Thermal properties and crystallinity of the ground PET and waste bottles PET (before and after reaction) samples were simultaneously analyzed using a TA instruments SDT Q600 (New Castle, DE, USA). Approximately 10 mg of sample was loaded on an aluminum crucible and heated from 25 to $800\text{ }^\circ\text{C}$ (TGA) and 25 to $300\text{ }^\circ\text{C}$ (DSC) at a heating rate of $10\text{ }^\circ\text{C min}^{-1}$ in N_2 . An empty aluminum crucible was used as reference. The percent crystallinity was calculated from cold crystallization (ΔH_{cc}) and heat of melting (ΔH_m) using eqn (9). The reference heat of melting (ΔH_m^0) for 100% crystalline PET is 140.1 J g^{-1} .⁵⁴

$$\text{Crystallinity}(\%) = \frac{\Delta H_m - \Delta H_{cc}}{\Delta H_m^0} \times 100 \quad (9)$$

2.6.3. Field emission scanning electron microscopy (FESEM). Pristine PET, subcritical $\text{CO}_2\text{-H}_2\text{O}$ and hot compressed H_2O (control)-treated PET samples were mounted on sticky carbon surface above the aluminum stubs and sputter coated 4 nm conductive Iridium using EMS150R S sputter coater (Electron Microscopy Sciences, USA). A S4700 II cFEG SEM (Hitachi High Technologies-America) was used to image the surface morphology of the samples. All the SEM data reported were collected at an acceleration voltage of 5 kV , and the images were obtained with a secondary electron detector.

3. Results and discussion

3.1. Effect of subcritical CO_2 loading on PET hydrolysis

To better understand the effect of the subcritical $\text{CO}_2\text{-H}_2\text{O}$ system on the hydrolysis of PET, a model substrate of semicrystalline, granulate ($3\text{--}5\text{ mm}$) PET was selected. Semicrystalline PET was expected to be more resistant to hydrolysis than amorphous PET (crystallinity acts as barrier to moisture and oxygen diffusion),⁵⁵ and thus semicrystalline PET can better highlight the relative robustness of the subcritical $\text{CO}_2\text{-H}_2\text{O}$ process toward highly crystalline substrates. Also, we have selected granulate PET due to the higher resistance to decomposition relative to powder, thus allowing for insights on potential mass transfer benefits of the use of subcritical $\text{CO}_2\text{-H}_2\text{O}$ system and its robustness. As a control experiment, hot com-



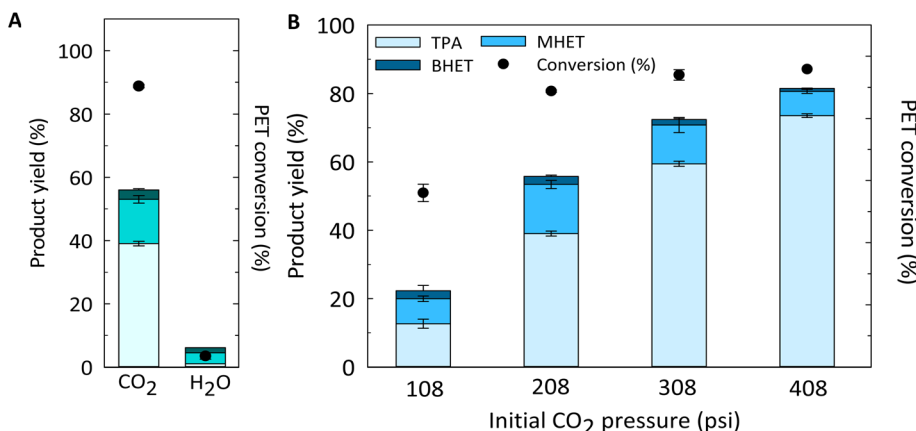


Fig. 1 Effect of CO₂ addition (A) and initial CO₂ pressure (B) on the hydrolysis of semicrystalline, granulate PET. Reaction conditions: PET to H₂O ratio 1:8 w/w (2.5 g PET : 20 mL H₂O), 180 °C, 208 psi of initial pressure (either CO₂ or N₂) for 100 min of residence time (A); PET to H₂O ratio 1:8 w/w (2.5 g PET : 20 mL H₂O), 180 °C for 100 min residence time (B). Reactions were conducted, at least, in duplicate, and error bars represent standard deviation. PET conversion is given as mass conversion into DMSO-soluble products.

pressed H₂O was used under 208 psi of initial N₂ pressure. Fig. 1 (and Table S1†) shows the effect of CO₂ *versus* N₂ (*i.e.* N₂-H₂O) control at 180 °C for 100 min. PET was almost completely converted to DMSO-soluble products (88.8 ± 0.5%), and a total product (TPA + MHET + BHET) yield of 55.7 ± 0.3% was reached. It is worth mentioning that intermediate compounds, such as dimers, were found at substantial levels after CO₂-H₂O reactions at 180 °C for 100 min (Fig. S1†). However, in the case of hot compressed H₂O, substantially lower PET depolymerization (and product formation) was observed. These results support the hypothesis that the dissolution of CO₂ in H₂O, and thus *in situ* formation of H₂CO₃ catalyzes the hydrolysis of PET ester bonds at 180 °C. It is challenging to compare the results obtained herein with those reported in the literature for neutral hydrolysis reactions, because of the wide variety of operational conditions reported and PET substrate properties/morphologies.^{13,16,56} Pereira *et al.* have reported a TPA yield <10% when PET chips from sparkling water bottles were hydrolyzed at 200 °C for 120 min.¹³ It is worth mentioning that when we performed hot compressed H₂O reactions (in the absence of N₂) a TPA yield <5% was observed at 200 °C for 100 min (Table S2†), which is in good agreement with the findings reported by Pereira *et al.* who did not use N₂ to pressurize the H₂O in those experiments.

The impact of CO₂ pressure (and composition) on the hydrolysis of PET was evaluated by varying initial CO₂ pressure before increasing temperature to 180 °C for 100 min of reaction time. As expected, increasing CO₂ pressures led to higher PET conversion into DMSO-soluble products and total product (*i.e.* TPA + MHET + BHET) yield (Fig. 1B). However, when the

initial CO₂ pressure was further increased to 408 psi, the total product (TPA + MHET + BHET) yield was only 12.7% higher than that obtained at 308 psi. To better understand the effect of CO₂ on product yield, we must understand the effect of varying CO₂ pressures on the pH of the system at a given reaction temperature and correlated with the obtained product yields. It is worth mentioning that the pH calculated herein does not include the contribution of the generated acidic products, such as TPA. The solubility of TPA in subcritical H₂O was measured by Takebayashi *et al.*, who reported that the mole fraction of TPA in H₂O varies from 0.610×10^{-3} and 1.77×10^{-3} at 174 and 200 °C, respectively.⁵⁷ Also, Yang *et al.* reported the hydrolysis of PET with TPA as a catalyst at 220 °C.⁵⁸ As shown in Fig. 2, an initial CO₂ pressure of 108 psi (calculated pH ~4.17) was sufficient to promote an acidity low enough to induce acid hydrolysis of PET into its constituents at 180 °C for 100 min. An increase of initial CO₂ pressure from 108 to 208 psi decreased the pH from 4.17 to 4.01, and this small difference in pH increased the TPA and MHET yields from $12.6 \pm 1.4\%$ to $39.1 \pm 0.7\%$ and 7.3 ± 0.8 to $14.3 \pm 1.2\%$, respectively. A further increase in CO₂ pressure from 308 to 408 psi only decreased the pH value from ~3.91 to 3.84, but allowed for MHET conversion to TPA resulting in a maximum TPA yield of $73.6 \pm 0.6\%$ at 180 °C for 100 min. These findings suggest that slight variations of pH in the medium are crucial to enhance hydrolysis of PET into TPA.

Additional experiments showed that an increase of PET and H₂O loadings (from 2.5 g PET : 20 mL H₂O to 3.75 g PET : 30 g H₂O), while keeping PET:H₂O ratio of 1:8 w/w constant, resulted in a substantial decrease in both PET conversion into DMSO-soluble products (from 99 to 37.5%) and TPA yield (from 85 to 7%) at 200 °C, 208 psi of initial CO₂ pressure for 100 min (Table S3†). In addition, at the same reaction conditions, when PET:H₂O ratios were changed from 1:5.3 to 1:8 w/w, while keeping the same H₂O amount (*i.e.*, from 3.75 g PET : 20 g H₂O to 2.5 g PET : 20 g H₂O), similar final



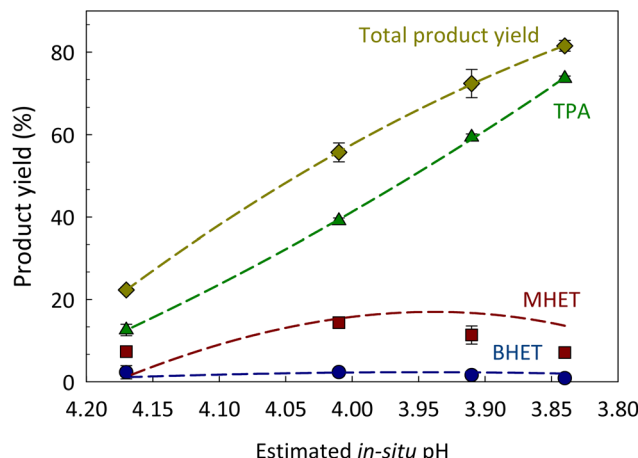


Fig. 2 Impact of CO_2 -induced pH (calculated using eqn (4)) on the yield of products. Reaction conditions: PET to H_2O ratio 1:8 w/w (2.5 g PET : 20 mL H_2O), 108 (estimated pH = 4.17), 208 (estimated pH = 4.01), 308 (estimated pH = 3.91) and 408 (estimated pH = 3.84) psi of initial CO_2 pressure at 180 °C for 100 min of reaction time. Lines were added to guide the eye. The estimated *in situ* pH did not include the contribution of other products (e.g., TPA) and assumed the system was under equilibrium.

pressures, PET conversion into DMSO-soluble products and TPA yield were observed. These results can be explained by the fact that the time required to reach equilibrium is highly dependent on the quantity of H_2O introduced into the system due to the diffusion limitation of CO_2 in the liquid phase. In other words, when the system is not under equilibrium conditions, the pH of the solution at reaction conditions will be less acidic. da Silva *et al.*, found that the performance of subcritical CO_2 - H_2O for hydrolyzing wheat straw was also impacted by the amount of H_2O added to the reactor.⁵⁹

3.2. Effect of reaction severity on PET hydrolysis

A series of reactions were conducted under variable conditions of temperature and residence time to assess the performance of subcritical CO_2 - H_2O to hydrolyze PET into TPA (Fig. 3A and Table S4†). The results show that increasing temperature favors the rate of conversion of PET to DMSO-soluble products (TPA + MHET + BHET). For example, a significant increase in total product yield was obtained for the first 40 min of reaction by only increasing temperature from 180 to 200 °C.

In addition, TPA was the main compound present in all reactions, except for the 10 min of reaction time. The amount of TPA recovered increased with both temperature and reaction time reaching a maximum of $85.0 \pm 1.3\%$ at 200 °C for 100 min. Under less severe conditions (e.g., 180 °C for 100 min and 190 °C for 40 min), BHET and MHET were found in appreciable amounts. This is expected, as BHET and MHET are reaction intermediates that are converted to TPA and EG over time. As shown here, every variable used in the system, notably temperature, CO_2 pressure and residence time, contributes in different ways to the severity of the reaction, which in turn impacts hydrolysis yields. Thus, the use of a combined severity factor (CS_{pCO_2}) was further evaluated to predict PET conversion into DMSO-soluble products and TPA yield upon CO_2 -aided hydrolysis.⁴⁷ The data obtained at temperatures ranging from 180 to 200 °C and from 10 to 100 min of reaction time (results from 180 to 200 °C for 10 min were not included due to negligible amount of TPA formed under those conditions) were used to evaluate the potential correlation between CS_{pCO_2} and TPA yield. As shown in Fig. 3B, the TPA yield correlates linearly ($R^2 = 0.977$) with CS_{pCO_2} , indicating that the effect of temperature, CO_2 pressure, and reaction time seem to be reasonably well expressed by the combined severity factor to predict TPA yields.

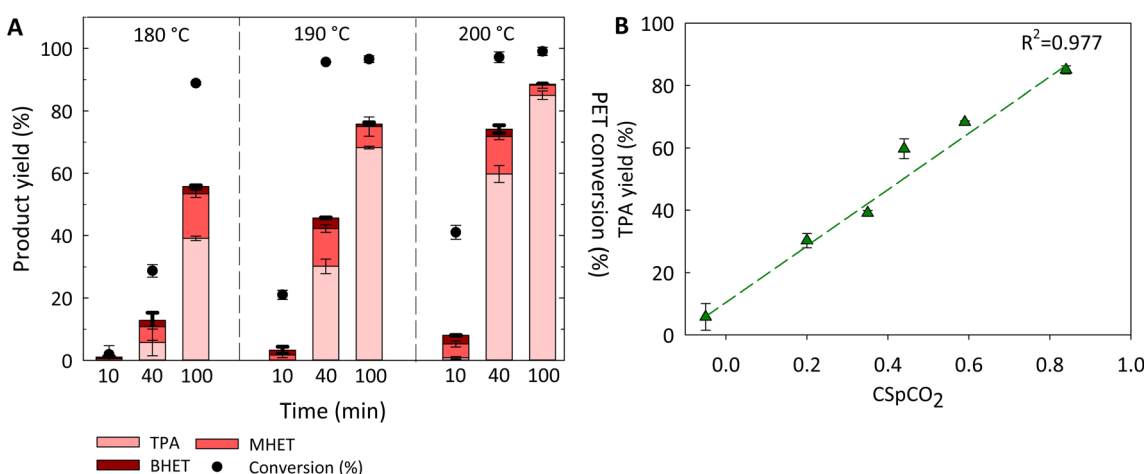


Fig. 3 Effect of temperature and reaction time on the performance of CO_2 - H_2O hydrolysis of PET (A). TPA yield as a function of combined severity factor (CS_{pCO_2}) (B). Reaction conditions: PET to H_2O ratio 1:8 w/w (2.5 g PET : 20 mL H_2O) and 208 psi of initial CO_2 pressure (A); PET to H_2O ratio 1:8 w/w (2.5 g PET : 20 mL H_2O) and 208 psi of initial CO_2 pressure at varying temperatures (180, 190 and 200 °C), and residence times (40 and 100 min) (B). Reactions were conducted, at least, in duplicate, and error bars represent standard deviation. The numerical values for both CS_{pCO_2} and TPA yield can be found in Table S4.† Fig. S3† shows the impact of CS_{pCO_2} on PET conversion. PET conversion is given as mass conversion into DMSO-soluble products.



3.3. Morphological characterization of leftover PET upon $\text{CO}_2\text{-H}_2\text{O}$ reaction

Characterization of morphological changes in the leftover PET samples (DMSO-insoluble) upon reactions in $\text{CO}_2\text{-H}_2\text{O}$ media would allow one to understand the effect of CO_2 addition to H_2O on the ultrastructure and possible disruption of the PET surface. Fig. 4 shows the SEM images of pristine PET and leftover PET after compressed hot H_2O ($\text{N}_2\text{-H}_2\text{O}$) and $\text{CO}_2\text{-H}_2\text{O}$ reactions at 165 °C in non-isothermal conditions. In addition, Fig. S2† shows additional SEM images of pristine and leftover PET samples after both hot compressed H_2O and subcritical $\text{CO}_2\text{-H}_2\text{O}$ process at varying operational conditions.

After $\text{CO}_2\text{-H}_2\text{O}$ process, the PET granulates seemed to clump together, and the PET surface appeared to be subjected to morphological changes (Fig. 4C). Both pristine PET and leftover PET after hot compressed H_2O treatment exhibited a tight and contiguous surface (Fig. 4A and B, respectively), while the PET after $\text{CO}_2\text{-H}_2\text{O}$ process showed irregular roughness and formation of pores (Fig. 4C). These morphological changes can be explained either by the polymer deconstruction or the

interaction between the polymer and CO_2 , and the enhanced diffusivity of CO_2 into the amorphous region of the substrate.

3.4. Assessment of subcritical $\text{CO}_2\text{-H}_2\text{O}$ process robustness

The development of recycling technologies that can effectively process plastics, regardless of the presence of incompatible polymers, fillers and additives (e.g., stabilizers, pigments and plasticizers) is critical for the commercial success of those technologies. Thus, the subcritical $\text{CO}_2\text{-H}_2\text{O}$ system was evaluated for the selective depolymerization of PET within a mixture of polymers (*i.e.*, HDPE + PET) and for the performance in recycling colored Canada Dry relative to transparent Pure Life® waste PET bottles.

A mixture composed of 50 : 50 w/w powder PET and HDPE and a substrate-to- H_2O ratio of 1 : 8 w/w (2.5 g substrate : 20 mL H_2O) was used to evaluate the selectivity of the proposed system for “molecular sorting” purposes. As can be seen in Fig. 5A (Table S5†), both total product and TPA yields obtained from the 50 : 50 w/w PET : PE powder mixture (PET and PE particle sizes were 300 and 150 μm , respectively) were very similar to the one obtained from pure 100% PET

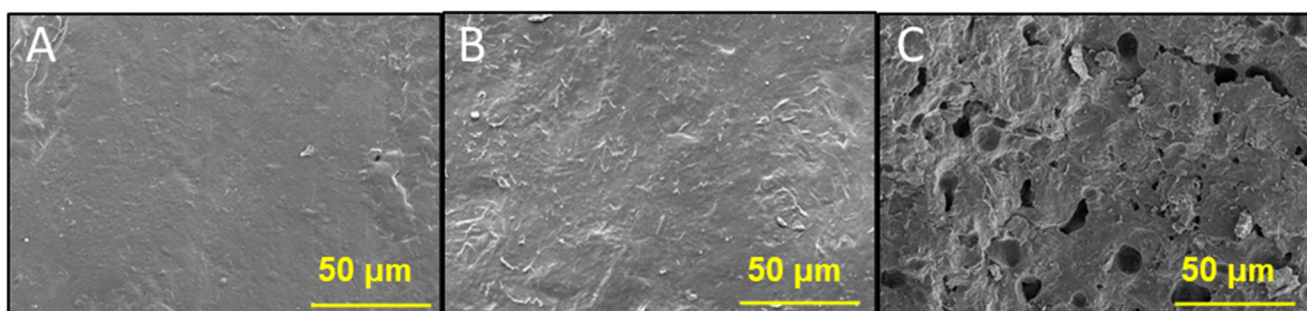


Fig. 4 Scanning electron microscopy of untreated, granulate PET (A), leftover PET samples from hot compressed H_2O (*i.e.* $\text{N}_2\text{-H}_2\text{O}$, with 208 psi of initial N_2 pressure) reaction (B), and $\text{CO}_2\text{-H}_2\text{O}$ reaction (208 psi of initial CO_2 pressure) (C) at 165 °C (non-isothermal conditions). Reaction conditions: PET to H_2O ratio 1 : 8 w/w (2.5 g PET : 20 mL H_2O).

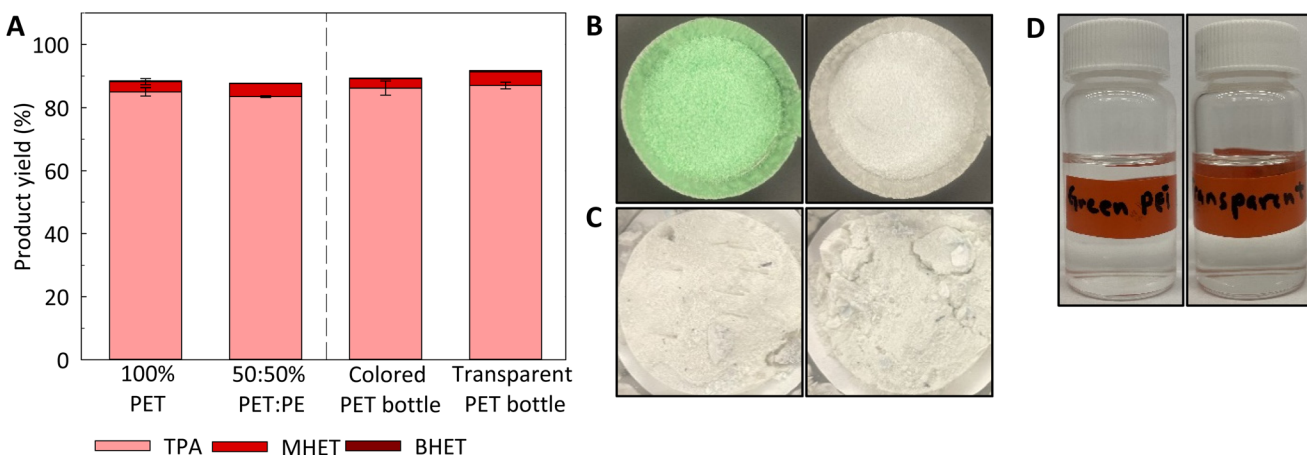


Fig. 5 Effect of subcritical $\text{CO}_2\text{-H}_2\text{O}$ on the hydrolysis of PET within 50 : 50 w/w PET-PE mixture and on colored Canada Dry and transparent Pure Life® PET bottles (A). Pristine colored Canada Dry and transparent Pure Life® PET soda bottles prior to reaction (B), H_2O -insoluble solids after reaction (including TPA, insoluble oligomers, additives and others) (C), and liquid product samples after filtration (D). Reaction conditions: Substrate to H_2O ratio 1 : 8 w/w (2.5 g substrate : 20 mL H_2O), 200 °C for 100 min and with an initial CO_2 pressure of 208 psi. Reactions were conducted, at least, in duplicate, and error bars represent standard deviation.



(300 μm) at 200 $^{\circ}\text{C}$ for 100 min. These findings were highly expected, as the operational conditions used herein do not promote the cleavage of C–C bonds in the HDPE, but are sufficient to promote the hydrolysis of ester bonds in PET. This shows that the performance of the subcritical CO_2 – H_2O process, at 200 $^{\circ}\text{C}$ for 100 min, does not seem to be impacted by the presence of other plastics and it can provide “molecular sorting” capabilities.

As shown in Table 1 and Fig. S4,† both colored Canada Dry and transparent Pure Life® PET bottles show similar crystallinity content and thermal stability after cryogrinding. Fig. 5A shows that there were no differences in total product yields between colored Canada Dry and transparent Pure Life® PET bottles upon CO_2 – H_2O processing under identical operational conditions. In addition, the green pigment initially present in the green Canada Dry soda bottle cannot be observed in the liquid product (Fig. 5D) nor in the leftover insoluble solids with the naked eye (Fig. 5C), resulting in a clean white product like that observed for the product derived from transparent PET bottle.

The chemical structure and purity of TPA recovered from colored waste PET bottle was compared with the TPA recovered from pristine PET through ^1H and ^{13}C NMR spectroscopy as shown in Fig. S5–S8.† As shown in Fig. S5 and S6,† ^1H NMR spectra of TPA produced from both standard PET and colored PET bottle showed two singlets with chemical shift at 8.0 and 13.3 ppm corresponding to the aromatic protons of the benzene ring and COOH proton, respectively.⁶⁰ Besides the peaks corresponding to DMSO-*d*6 (2.50 ppm) and H_2O (3.38 ppm), no other significant peaks were observed in both ^1H NMR spectra. ^{13}C NMR spectra of TPA from both standard PET and colored Canada Dry PET bottle showed three main peaks corresponding to aromatic carbon (130.1 ppm), quaternary aromatic carbon (135.0 ppm) and carbonyl carbon (167.1 ppm) atoms of TPA (Fig. S7 and S8†).⁶¹ The absence of other peaks in both ^1H NMR and ^{13}C NMR indicate that subcritical CO_2 – H_2O is able to produce TPA with high purity. We further investigated the performance of the CO_2 – H_2O process in hydrolyzing other colored waste PET bottles (*i.e.*, Mountain Dew and Twist Up) (Tables S5, S6, and Fig. S9, S10†) at the same operational conditions, and similar results to colored Canada Dry PET bottle has been obtained (Table S5†). Although the pigments present in the colored PET bottles have been reported to contain somewhat acidic compounds,⁶² they did not significantly impact the performance of subcritical CO_2 – H_2O process at the studied conditions. The reason for the discoloration of the reaction products after subcritical CO_2 –

Table 1 Crystallinity content, enthalpy of melting (ΔH_m), cold crystallization enthalpy (ΔH_{cc}) of colored and noncolored PET soda bottles used in this work

| Substrate | Crystallinity (%) | ΔH_m (J g $^{-1}$) | ΔH_{cc} (J g $^{-1}$) |
|-----------------------------------|-------------------|-----------------------------|--------------------------------|
| Colored Canada Dry PET bottle | 17.9 ± 0.5 | 25.0 ± 0.7 | 0 |
| Transparent Pure Life® PET bottle | 20.6 ± 0.1 | 29.1 ± 0.0 | 0 |

H_2O exposure is still unknown, as the chemical nature of the green dye in the commercial PET bottles has not been reported by the manufacturer. However, we hypothesize that the dye is susceptible to chemical change when exposed to the conditions present in the media during CO_2 – H_2O processing.

4. Conclusions

This work shows the potential of adding subcritical CO_2 to the aqueous hydrolysis of PET. The subcritical CO_2 – H_2O process resulted in a TPA yield of $39.1 \pm 0.7\%$ (*versus* $1.7 \pm 0.4\%$ obtained in hot H_2O control reaction) at 180 $^{\circ}\text{C}$, PET : H_2O loading of 2.5 g PET : 20 g H_2O for 100 min. At 200 $^{\circ}\text{C}$ for 100 min, a TPA yield of $85.0 \pm 1.3\%$ was achieved. In addition, the performance of subcritical CO_2 – H_2O was not impacted by the presence of polyolefins within the mixture and/or pigments present in waste PET bottles.

Author contributions

Funding acquisition – ARCM; conceptualization – ARCM, DO, LG; investigation – DO, LG, AS, JM, CL; methodology – DO, LG, ARCM; supervision – LG, ARCM, NAR; visualization – DO, ARCM; writing – original draft – DO, ARCM; writing – review & editing – DO, LG, AS, JM, CL, NAR, ARCM.

Conflicts of interest

There are no conflicts of interest to declare.

Acknowledgements

This material is based upon work supported by the National Science Foundation under Grant No. OIA – 2119754, and by the Kansas Board of Regents EPSCoR Grant Program. Also, the authors are grateful to the Department of Chemical and Petroleum Engineering, and the School of Engineering at University of Kansas for their financial support. The authors gratefully acknowledge Dr Erhan Demirel from the Institute for Bioengineering Research (University of Kansas) and Dr Anoop Uchagawkar from Center for Environmental and Beneficial Catalysis (CEBC) (University of Kansas) for their assistance in acquiring and analyzing the DSC data. The authors also thank the access to the medicinal chemistry laboratory at the University of Kansas for LC-MS analysis provided by Samuel Gary and Dr Steven Bloom. We thank Dr Prem Thapa-Chetri from the Microscopy and Analytical Imaging Lab (University of Kansas) for his assistance collecting SEM data. This work was authored in part by the National Renewable Energy Laboratory, operated by Alliance for Sustainable Energy, LLC, for the U.S. Department of Energy (DOE) under Contract No. DE-AC36-08GO28308. C. L. and N. A. R. were funded by the U.S. Department of Energy, Office of Energy

Efficiency and Renewable Energy, Advanced Materials and Manufacturing Technologies Office (AMMTO) and Bioenergy Technologies Office (BETO). This work was performed as part of the BOTTLE™ Consortium and was supported by AMMTO and BETO under contract no. DE-AC36-08GO28308 with the National Renewable Energy Laboratory, operated by Alliance for Sustainable Energy, LLC. The views expressed in the article do not necessarily represent the views of the DOE or the U.S. Government. The U.S. Government retains and the publisher, by accepting the article for publication, acknowledges that the U.S. Government retains a nonexclusive, paid-up, irrevocable, worldwide license to publish or reproduce the published form of this work, or allow others to do so, for U.S. Government purposes.

References

- 1 A. Bescond and A. Pujari, PET polymer, in *Chemical Economics Handbook (IHS, Markit)*, 2020, p. 32. <https://ihsmarkit.com/products/chemical-economics-handbooks.html>.
- 2 E. Ormonde, U. Loechner, M. Yoneyama and X. Zhu, *Plastics recycling – Chemical Economics Handbook (IHS Markit)*, 2022, p. 56. <https://www.spglobal.com/commodityinsights/en/ci/products/plastics-recycling-chemical-economics-handbook.html>.
- 3 A. Rahimi and J. M. García, *Nat. Rev. Chem.*, 2017, **1**, 0046.
- 4 V. Sinha, M. R. Patel and J. V. Patel, *J. Polym. Environ.*, 2010, **18**, 8–25.
- 5 D. Paszun and T. Spychaj, *Ind. Eng. Chem. Res.*, 1997, **36**, 1373–1383.
- 6 T. E. Long and J. Scheirs, *Modern polyesters: chemistry and technology of polyesters and copolyesters*, John Wiley & Sons, 2005.
- 7 T. Yoshioka, T. Motoki and A. Okuwaki, *Ind. Eng. Chem. Res.*, 2001, **40**, 75–79.
- 8 T. Yoshioka, N. Okayama and A. Okuwaki, *Ind. Eng. Chem. Res.*, 1998, **37**, 336–340.
- 9 S. Mishra, A. Goje and V. Zope, *Polym. React. Eng.*, 2003, **11**, 79–99.
- 10 M. J. Kang, H. J. Yu, J. Jegal, H. S. Kim and H. G. Cha, *Chem. Eng. J.*, 2020, **398**, 125655.
- 11 E. Barnard, J. J. R. Arias and W. Thielemans, *Green Chem.*, 2021, **23**, 3765–3789.
- 12 A. Jaime-Azuara, T. H. Pedersen and R. Wimmer, *Green Chem.*, 2023, **25**, 2711–2722.
- 13 P. Pereira, P. E. Savage and C. W. Pester, *ACS Sustainable Chem. Eng.*, 2023, **11**, 7203–7209.
- 14 C. Schacht, C. Zetzl and G. Brunner, *J. Supercrit. Fluids*, 2008, **46**, 299–321.
- 15 W. L. Marshall and E. Franck, *J. Phys. Chem. Ref. Data*, 1981, **10**, 295–304.
- 16 C. N. Onwucha, C. O. Ehi-Eromosele, S. O. Ajayi, M. Schaefer, S. Indris and H. Ehrenberg, *Ind. Eng. Chem. Res.*, 2023, **62**, 6378–6385.
- 17 J. R. Campanelli, M. Kamal and D. Cooper, *J. Appl. Polym. Sci.*, 1993, **48**, 443–451.
- 18 M. Han, in *Recycling of Polyethylene Terephthalate Bottles*, Elsevier, 2019, pp. 85–108.
- 19 V. S. Zope and S. Mishra, *J. Appl. Polym. Sci.*, 2008, **110**, 2179–2183.
- 20 A. R. C. Morais, A. M. da Costa Lopes and R. Bogel-Lukasik, *Chem. Rev.*, 2015, **115**, 3–27.
- 21 D. Damayanti, B. T. Basae, L. Al Mukarromah, D. S. S. Marpaung, D. R. Saputri, A. Sanjaya, Y. Fahni, D. Supriyadi, T. Taharuddin and H. S. Wu, *Clean. Eng. Technol.*, 2023, 100697.
- 22 S. P. Nalawade, F. Picchioni and L. Janssen, *Prog. Polym. Sci.*, 2006, **31**, 19–43.
- 23 X. Gao, Y. Chen, P. Chen, Z. Xu, L. Zhao and D. Hu, *J. CO2 Util.*, 2022, **57**, 101887.
- 24 I. Elmanovich, A. Stakhanov, E. Kravchenko, S. Stakhanova, A. Pavlov, M. Ilyin, E. Kharitonova, M. Gallyamov and A. Khokhlov, *J. Supercrit. Fluids*, 2022, **181**, 105503.
- 25 R. Wissinger and M. Paulaitis, *J. Polym. Sci., Part B: Polym. Phys.*, 1987, **25**, 2497–2510.
- 26 M. Champeau, J.-M. Thomassin, C. Jérôme and T. Tassaing, *J. Supercrit. Fluids*, 2014, **90**, 44–52.
- 27 I. Kikic and F. Vecchione, *Curr. Opin. Solid State Mater. Sci.*, 2003, **7**, 399–405.
- 28 Z. Zhang and Y. P. Handa, *J. Polym. Sci., Part B: Polym. Phys.*, 1998, **36**, 977–982.
- 29 S. G. Kazarian, N. H. Brantley and C. A. Eckert, *Vib. Spectrosc.*, 1999, **19**, 277–283.
- 30 M. Takada and M. Ohshima, *Polym. Eng. Sci.*, 2003, **43**, 479–489.
- 31 S. Lambert and M. Paulaitis, *J. Supercrit. Fluids*, 1991, **4**, 15–23.
- 32 J. Liu and J. Yin, *Ind. Eng. Chem. Res.*, 2022, **61**, 6813–6819.
- 33 W.-Z. Guo, H. Lu, X.-K. Li and G.-P. Cao, *RSC Adv.*, 2016, **6**, 43171–43184.
- 34 K. Yu, J. Liu, J. Sun, Z. Shen and J. Yin, *J. Supercrit. Fluids*, 2023, **194**, 105837.
- 35 Y. Li, M. Wang, X. Liu, C. Hu, D. Xiao and D. Ma, *Angew. Chem.*, 2022, **134**, e202117205.
- 36 Y. Yang, S. Sharma, C. Di Bernardo, E. Rossi, R. Lima, F. S. Kamounah, M. Poderyte, K. Enemark-Rasmussen, G. Ciancaleoni and J.-W. Lee, *ACS Sustainable Chem. Eng.*, 2023, **11**, 11294–11304.
- 37 X. K. Li, H. Lu, W. Z. Guo, G. P. Cao, H. L. Liu and Y. H. Shi, *AIChE J.*, 2015, **61**, 200–214.
- 38 S. E. Hunter and P. E. Savage, *AIChE J.*, 2008, **54**, 516–528.
- 39 A. R. C. Morais, A. C. Mata and R. Bogel-Lukasik, *Green Chem.*, 2014, **16**, 4312–4322.
- 40 D. H. Fockink, A. R. C. Morais, L. P. Ramos and R. M. Lukasik, *Energy*, 2018, **151**, 536–544.
- 41 A. Toscan, A. R. C. Morais, S. M. Paixão, L. Alves, J. r. Andreaus, M. Camassola, A. J. P. Dillon and R. M. Lukasik, *Ind. Eng. Chem. Res.*, 2017, **56**, 5138–5145.



42 A. R. C. Morais, M. D. D. Matuchaki, J. Andreaus and R. Bogel-Lukasik, *Green Chem.*, 2016, **18**, 2985–2994.

43 A. R. C. Morais and R. Bogel-Lukasik, *Green Chem.*, 2016, **18**, 2331–2334.

44 J. S. Luterbacher, J. W. Tester and L. P. Walker, *Biotechnol. Bioeng.*, 2010, **107**, 451–460.

45 J. S. Luterbacher, J. W. Tester and L. P. Walker, *Biotechnol. Bioeng.*, 2012, **109**, 1499–1507.

46 J. S. Luterbacher, Q. Chew, Y. Li, J. W. Tester and L. P. Walker, *Energy Environ. Sci.*, 2012, **5**, 6990–7000.

47 G. P. Van Walsum, in *Severity function describing the hydrolysis of xylan using carbonic acid*, Twenty-Second Symposium on Biotechnology for Fuels and Chemicals, Springer, 2001, pp. 317–329.

48 R. P. Overend and E. Chornet, *Philos. Trans. R. Soc., A*, 1987, **321**, 523–536.

49 D. H. Fockink, J. H. Sánchez and L. P. Ramos, *Ind. Crops Prod.*, 2018, **123**, 563–572.

50 A. R. Abouelela, P. Y. Nakasu and J. P. Hallett, *ACS Sustainable Chem. Eng.*, 2023, **11**, 2404–2415.

51 A. Toscan, A. R. C. Morais, S. M. Paixão, L. Alves, J. Andreaus, M. Camassola, A. J. P. Dillon and R. M. Lukasik, *Bioresour. Technol.*, 2017, **224**, 639–647.

52 S. Kaabel, J. D. Therien, C. E. Deschênes, D. Duncan, T. Friščić and K. Auclair, *Proc. Natl. Acad. Sci. U. S. A.*, 2021, **118**, e2026452118.

53 S. Mori and H. G. Barth, *Size exclusion chromatography*, Springer Science & Business Media, 1999.

54 A. Mehta, U. Gaur and B. Wunderlich, *J. Polym. Sci., Polym. Phys. Ed.*, 1978, **16**, 289–296.

55 N. S. Allen, M. Edge, M. Mohammadian and K. Jones, *Eur. Polym. J.*, 1991, **27**, 1373–1378.

56 H. Abedsoltan, Z. Zoghi and A. H. Mohammadi, *J. Appl. Polym. Sci.*, 2023, e53949.

57 Y. Takebayashi, K. Sue, S. Yoda, Y. Hakuta and T. Furuya, *J. Chem. Eng. Data*, 2012, **57**, 1810–1816.

58 W. Yang, R. Liu, C. Li, Y. Song and C. Hu, *Waste Manage.*, 2021, **135**, 267–274.

59 S. P. M. da Silva, A. R. C. Morais and R. Bogel-Lukasik, *Green Chem.*, 2014, **16**, 238–246.

60 V. Štrukil, *ChemSusChem*, 2021, **14**, 330–338.

61 R. Pétiaud, H. Waton and Q.-T. Pham, *Polymer*, 1992, **33**, 3155–3161.

62 K. Fukushima, D. J. Coady, G. O. Jones, H. A. Almegren, A. M. Alabdulrahman, F. D. Alsewailem, H. W. Horn, J. E. Rice and J. L. Hedrick, *J. Polym. Sci., Part A: Polym. Chem.*, 2013, **51**, 1606–1611.

